JGR Oceans

RESEARCH ARTICLE
10.1029/2018JC014603

Long-Term Trend of the Tropical Pacific Trade Winds Under Global Warming and Its Causes

Yang Li[1], Quanliang Chen[1], Xiaoran Liu[2], Jianping Li[3], Nan Xing[4], Fei Xie[5], Juan Feng[5], Xin Zhou[1], Hongke Cai[1], and Zhenglin Wang[1]

[1]College of Atmospheric Science, Plateau Atmosphere and Environment Key Laboratory of Sichuan Province, Chengdu University of Information Technology, Chengdu, China, [2]Chongqing Climate Center, Chongqing, China, [3]Key Laboratory of Physical Oceanography, Institute for Advanced Ocean Studies, Ocean University of China and Qingdao National Laboratory for Marine Science and Technology, Qingdao, China, [4]Beijing Municipal Weather Forecast Center, Beijing, China, [5]College of Global Change and Earth System Sciences, Beijing Normal University, Beijing, China

Key Points:
- There is the strengthening trend of the trades in the western equatorial Pacific and weakening trend in the eastern equatorial Pacific
- This long-term trend pattern can be primarily attributed to the CTM rather than to the impact of ENSO, El Niño Modoki, or IPO
- Based on the Gill-Matsuno theory, the long-term trend of the CTM can induce the long-term trend of trade winds

Correspondence to:
Q. Chen,
chenql@cuit.edu.cn

Citation:
Li, Y., Chen, Q., Liu, X., Li, J., Xing, N., Xie, F., et al. (2019). Long-term trend of the tropical Pacific trade winds under global warming and its causes. *Journal of Geophysical Research: Oceans*, *124*, 2626–2640. https://doi.org/10.1029/2018JC014603

Received 1 OCT 2018
Accepted 10 MAR 2019
Accepted article online 13 MAR 2019
Published online 14 APR 2019

Abstract The recent intensification of trade winds over the tropical Pacific is the strongest ever observed in the past hundred years. This strengthening trend is of great interest in recent research, but the causes are still unclear. Using two relatively long-term surface wind data sets, the present research shows that there is an overall strengthening trend of the trades in the western equatorial Pacific and an overall weakening trend in the eastern equatorial Pacific. This long-term trend pattern can be primarily attributed to the cold tongue mode (CTM) rather than to the impact of El Niño–Southern Oscillation (ENSO), El Niño Modoki, or Interdecadal Pacific Oscillation (IPO). The CTM, the second empirical orthogonal function mode of the sea surface temperature anomalies (SSTA) in the tropical Pacific, represents a strong long-term trend of tropical Pacific background state under global warming. According to the Gill-Matsuno theory, the easterly winds over the western equatorial Pacific are induced by the equatorial Pacific cooling and warming SSTA associated with the CTM, while the westerly winds over the eastern equatorial Pacific is primarily due to the eastern equatorial Pacific cooling SSTA associated with the CTM. Ultimately, an alternative explanation of past and future changes of the trades is expected to lead to improved understanding of the global climatic impacts of the enhanced trades in tropical Pacific under global warming.

1. Introduction

The trade winds over the tropical Pacific play an important role in global climate change. For example, the trade winds modulate the El Niño–Southern Oscillation (ENSO) cycle via the Bjerknes feedback (e.g., Battisti & Hirst, 1989, Bjerknes, 1969, Jin, 1997a, 1997b, Ren & Jin, 2013, Suarez & Schopf, 1988, Zheng et al., 2014, 2016); enhanced trade winds transport and converge moisture into the Eastern Hemisphere monsoon regions, which leads to increased global monsoon precipitation (Wang et al., 2012); and the trade winds play an important role in the Asian-Australian monsoon system (e.g., Li et al., 2011; Li & Zhang, 2008; Yang et al., 2017; Yang et al., 2017), American monsoon system (e.g., Vera et al., 2006), and ENSO diversity (e.g., Chen et al., 2015, Lian et al., 2014). Recently, Boisséson et al. (2014) showed that the strengthening of trade winds over the Pacific is a robust feature in several observational data sets as well as in reanalyses based on full and limited sets of observations. Particularly, the recent intensification of trade winds is the strongest ever observed in the past hundred years (e.g., Takahashi & Watanabe, 2016). There is a widespread view that the strengthening trade winds are associated with various interesting phenomena such as the global warming hiatus (e.g., Kosaka & Xie, 2013; Trenberth & Fasullo, 2013) and increased ocean heat uptake (e.g., Balmaseda et al., 2013, England et al., 2014). Therefore, understanding of the strengthening of the trade winds is of great importance for understanding air-sea interaction in the tropical Pacific, ENSO diversity, the global monsoon, and global warming. However, the causes of the strengthening trade winds are still unclear (e.g., Takahashi & Watanabe, 2016).

Recent studies have suggested that the strengthening trade winds may be explained by the natural internal variability in the Pacific, such as the El Niño Modoki (EM; e.g., Sohn et al., 2013), the Interdecadal Pacific Oscillation (IPO; e.g., Dong & Zhou, 2014, England et al., 2014, Ma & Zhou, 2016), and the centennial-scale variability (e.g., Giese & Ray, 2011; Ray & Giese, 2012). The EM (Ashok et al., 2007), also referred to the dateline El Niño (Larkin & Harrison, 2005), Central Pacific El Niño (Kao & Yu, 2009), or warm pool El Niño

(Kug et al., 2009), has become increasingly common in the past three decades (e.g., Ashok et al., 2007; Ding et al., 2015; Ding et al., 2015; Feng & Li, 2011; Feng & Li, 2013; Kao & Yu, 2009; Karnauskas, 2013; Kug et al., 2009; Ren et al., 2013; Ren & Jin, 2011; Takahashi et al., 2011; Zhang et al., 2011; Zhang et al., 2013, 2014). The EM is characterized by maximum sea surface temperature anomaly (SSTA) in the central equatorial Pacific, while the maximum SSTA in a conventional El Niño is located in the eastern equatorial Pacific. McPhaden et al. (2011) argued that the asymmetric spatial structures of these two different El Niño events could modulate the tropical Pacific mean state and thus explain the recent cooling SSTA in the eastern tropical Pacific. Furthermore, Sohn et al. (2013) pointed out that the recent more frequent occurrences of EM events intensified the Walker circulation and thus enhanced trade winds over the equatorial Pacific. Meanwhile, England et al. (2014) suggested that the recent IPO variability may have enhanced the trade winds over the tropical Pacific. In addition, Giese and Ray (2011) and Ray and Giese (2012) argued a centennial modulation in the strength of El Niño from late nineteenth century to late twentieth century. This indicates that the centennial-scale variability may contribute to the trades trend, because the zonal SST gradient over the tropical Pacific are crucial in determining Walker circulation or trades trend (e.g., Meng et al., 2012, Sandeep et al., 2014).

Although there is uncertainty at the beginning of the century due to the lower observational density in the earlier part of the record (e.g., Compo et al., 2011), the strengthening trend of Pacific Walker circulation or trades since 1950 is a robust feature in multiple data sets (e.g., L'Heureux et al., 2013) and its associated increasing trend of zonal SST gradient over the equatorial Pacific since 1900 has also been found in multiple observational data sets (e.g., Cane et al., 1997, Li et al., 2017, Solomon & Newman, 2012). Particularly, many studies have reported that the intensification of the tropical Pacific trade winds over the past two decades is the strongest in the past century (e.g., Boisséson et al., 2014; England et al., 2014; L'Heureux et al., 2013; Takahashi & Watanabe, 2016). These results suggested that natural internal variability alone may not explain the strengthening trade winds.

Some studies have also emphasized the important role of external forcing in the strengthening of trade winds in the tropical Pacific (e.g., L'Heureux et al., 2013; Li & Ren, 2012; Zhang & Karnauskas, 2016). For example, L'Heureux et al. (2013) found a strengthened Walker circulation using 10 different sea level pressure data sets. They further pointed out that the intensification of the Walker circulation is associated with the La Niña-like pattern of the long-term trend of tropical Pacific SSTA, with greater cooling SSTA in the eastern tropical Pacific than in the west. Although there are large discrepancies between the various estimates of long-term change in the tropical Pacific under global warming (e.g., Collins et al., 2010, Vecchi et al., 2008), many observations have confirmed that the long-term trend of tropical Pacific SSTA is characterized by cooling in the eastern equatorial Pacific and warming elsewhere in the tropical Pacific (i.e., a La Niña-like pattern; e.g., Cane et al., 1997, Coats & Karnauskas, 2017, Compo & Sardeshmukh, 2010, Funk & Hoell, 2015, Karnauskas et al., 2009, Li et al., 2015, Li et al., 2017, Solomon & Newman, 2012, Zhang et al., 2010). Furthermore, the accelerating equatorial undercurrent, accelerating subtropical cells in the tropical Pacific, and the subsurface cooling in the eastern equatorial Pacific associated with the La Niña-like pattern have also been found in multiple observational data sets (e.g., Drenkard & Karnauskas, 2014, Li et al., 2017, Yang et al., 2014). In particular, the La Niña-like pattern in the tropical Pacific is dominated by ocean dynamical process, whereby vigorous upwelling of cold water in the eastern equatorial region causes the slower warming in the eastern Pacific than in the western Pacific (e.g., Cane et al., 1997; Clement et al., 1996; DiNezio et al., 2009; Karnauskas et al., 2009; Li et al., 2015, 2017; Seager & Murtugudde, 1997; Sun & Liu, 1996; Zhang et al., 2010).

The above studies (e.g., Dong & Zhou, 2014; England et al., 2014; L'Heureux et al., 2013; Li & Ren, 2012; Ma & Zhou, 2016; Sohn et al., 2013; Zhang & Karnauskas, 2016) suggested that natural internal variability and global warming can both contribute to the long-term trend of the trade winds. However, it is not yet clear which plays the major role. And, whether the long-term trend of the trade winds along the equatorial Pacific is strengthening uniformly is still pending. Therefore, the primary objective of the present study is to analyze the long-term trend of tropical Pacific trade winds and to understand the fundamental drivers of this long-term trend. Efforts are made to address the following specific questions: What is the long-term trend of trade winds over the tropical Pacific? What are the causes of the trends, if they exist? These questions are discussed in section 3. Section 2 briefly introduces the observational data sets and methods. Conclusions and a discussion are presented in section 4.

2. Data, Indices, and Methodology

2.1. Data

We used two relatively long-record surface wind data sets to investigate the long-term trend of the tropical Pacific trade winds. The first is the European Centre for Medium-Range Weather Forecasts (ECMWF)'s atmospheric reanalysis of the 20th Century (ERA20C), and the second is the Twentieth Century Reanalysis Version 2 (20CR2). Furthermore, previous studies have showed that the trade winds of the ERA20C and 20CR2 data sets are highly consistent with those of the ERA-Interim data sets (e.g., Boisséson et al., 2014, England et al., 2014). The ERA20C data set with 1.0° × 1.0° horizontal resolution covers the period 1900–2010 (Poli et al., 2016). Its observations assimilated include surface pressure from the International Surface Pressure Databank-Version 3.2.6 and ICOADS Version 2.5.1 and surface wind over the oceans from ICOADS Version 2.5.1. The 20CR2 data set with 2.0° × 2.0° horizontal resolution covers the period 1871–2012 (Compo et al., 2011). This data set is a comprehensive global atmospheric circulation data set and contains a synoptic-observation-based estimate of global tropospheric variability. In this study, the overlapping period (i.e., 1900–2010) of the ERA20C and 20CR2 data sets is used to study the long-term trend of the tropical Pacific trade winds. In addition, the monthly SST data set used in this study is the UK Met Office Hadley Centre Sea Ice and SST version 1 (HadISST1), whose horizontal resolution is 1.0° × 1.0° (Rayner et al., 2003). Also used is the fourth UK Met Office Hadley Centre and Climatic Research Unit Global Land and Sea Surface Temperature Data Set (HadCRUT4) on a 5° × 5° grid (Morice et al., 2012). Note that the mean seasonal cycle of all data sets from 1961 to 1990 has been removed.

2.2. Indices

The monthly Niño 3 index (5°S–5°N, 150°W–90°W), the EM index (hereafter EMI), and the IPO index are used in this study. Following Ashok et al. (2007), the EMI is defined as follows:

$$\mathrm{EMI} = [\mathrm{SSTA}]_C - 0.5[\mathrm{SSTA}]_E - 0.5[\mathrm{SSTA}]_W, \tag{1}$$

where square brackets with a subscript represent the area-mean SSTA over the central Pacific region (C: 10°S–10°N, 165°E–140°W), eastern Pacific region (E: 15°S–5°N, 110°–70°W), and western Pacific region (W: 10°S–20°N, 125–145°E).

Following Henley et al. (2015), the tripole index for the IPO is based on the difference between the SSTA averaged over the central equatorial Pacific and the average of the SSTA in the northwest and southwest Pacific. The tripole index is defined as follows:

$$\mathrm{TPI} = [\mathrm{SSTA}]_2 - \frac{[\mathrm{SSTA}]_1 + [\mathrm{SSTA}]_3}{2}, \tag{2}$$

where square brackets with a subscript represent the area-mean SSTA over region 1 (25°S–45°N, 140°E–145°W), region 2 (10°S–10°N, 170°E–90°W), and region 3 (W: 50°S–15°N, 150°E–160°W).

2.3. Methodology

Several statistical methods were used in this study. The primary method is trend analysis. Trends were calculated as the Theil-Sen median slope (Sen, 1968; Theil, 1950) and tested for statistical significance using the Mann-Kendall test. Note that the Theil-Sen trend estimation method is insensitive to outliers and is measured by the median of slopes between all pairs. The Theil-Sen trend was determined by the following equation:

$$\mathrm{trend} = \mathrm{Median}\left(\frac{x_i - x_j}{i - j}\right), \quad \forall j < i, 1 \le j < i \le N \tag{3}$$

where trend is the Theil-Sen trend, x_i and x_j are one data pair, and N is the sample size.

Correlation and regression methods were also used in this study. The statistical significance of the correlation between two autocorrelated time series was calculated using the two-tailed Student's t test and the

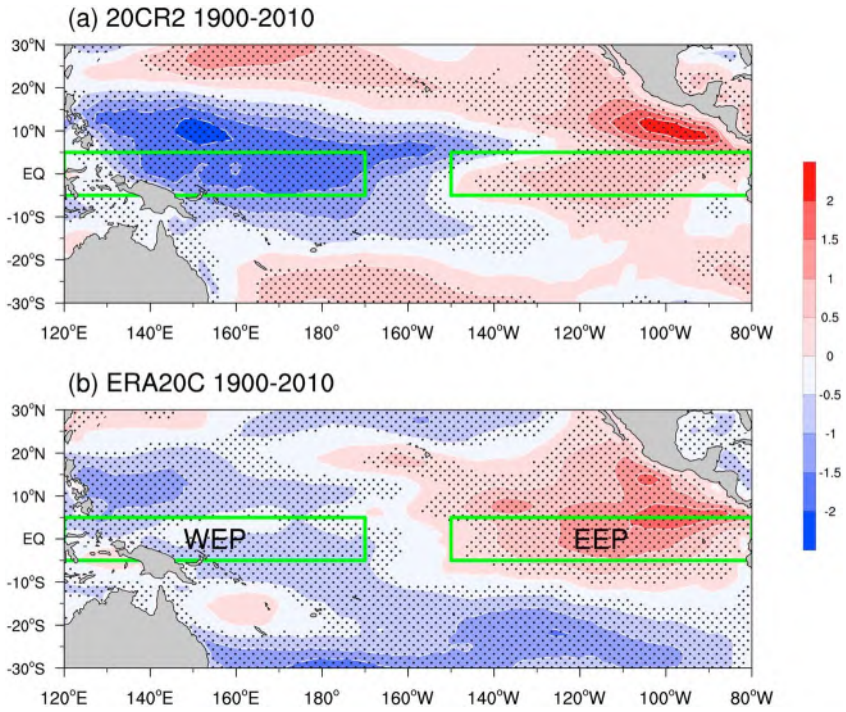

Figure 1. Trends of the tropical Pacific zonal wind anomalies (in m/s per 100 years) from 1900 to 2010 in (a) 20CR2 and (b) ERA20C. Stippled regions indicate statistical significance at the 99% confidence level. The two areas are the western equatorial Pacific (WEP; 5°S–5°N, 120°E–170°W) and the eastern equatorial Pacific (EEP; 5°S–5°N, 150–80°W).

effective number (N^{eff}) of degrees of freedom (Bretherton et al., 1999). For this study, N^{eff} was determined by the following approximation (e.g., Li et al., 2012; Li et al., 2013; Xie et al., 2016, 2017):

$$\frac{1}{N^{\text{eff}}} \approx \frac{1}{N} + \frac{2}{N}\sum_{j=1}^{N}\frac{N-j}{N}\rho_{XX}(\mathrm{j})\rho_{YY}(\mathrm{j}), \tag{4}$$

where N is the sample size and ρ_{XX} and ρ_{YY} are the autocorrelations of two sampled time series, X and Y, respectively, at time lag j.

3. Results

3.1. Long-Term Trend of the Tropical Pacific Trades

What is the long-term trend of trade winds over the tropical Pacific? Figure 1 shows the long-term trend of the tropical Pacific zonal wind anomalies based on two different data sets (i.e., 20CR2 and ERA20C). In spite of some differences, these two data sets exhibit similar long-term trend patterns of trade winds (Figure 1). That is, there is an overall strengthening trend of trades in the western equatorial Pacific and overall weakening trend in the eastern equatorial Pacific. Note that the trend distribution of these two data sets during the presatellite/postsatellite era (not shown) is consistent with that of their covering period (Figure 1). This is an interesting trend pattern (Figure 1), because previous studies emphasized the strengthening trades over the whole equatorial Pacific (e.g., England et al., 2014).

To reveal more clearly the long-term trends, the zonal wind anomalies averaged over the western equatorial Pacific (WEP; 5°S–5°N, 120°E–170°W) and over the eastern equatorial Pacific (EEP; 5°S–5°N, 150°W–80°W) are also investigated. Figure 2 shows the time series of zonal wind anomalies averaged over the WEP (hereafter U_{WEP}) and EEP (U_{EEP}) for the 20CR2 and ERA20C data sets. There is strong correlation between the two data sets for raw U_{WEP} time series (correlation coefficient r about 0.75) but relatively low correlation for raw U_{EEP} time series (r about 0.62; Figures 2a and 2b). Note that the uncertainty associated with the relatively sparse observations over the early part of the analysis period may reduce the correlation

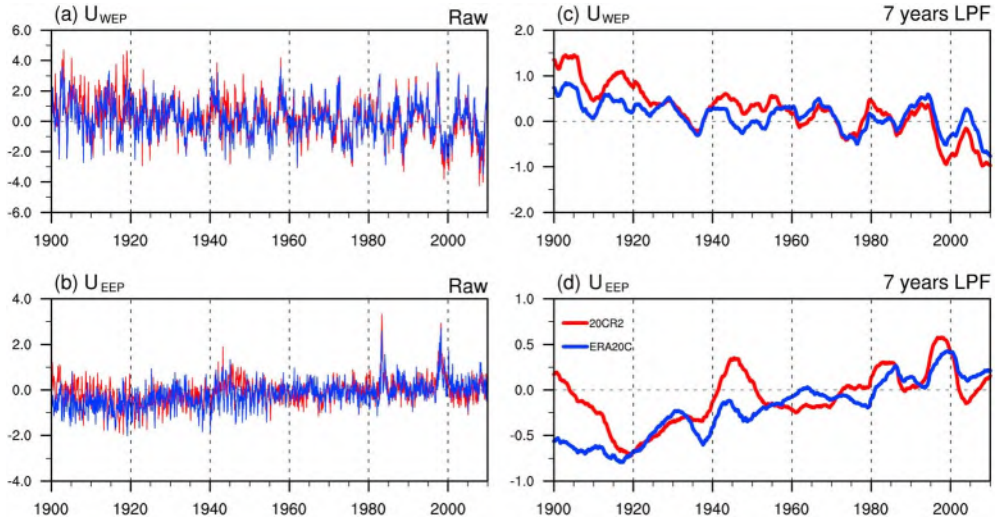

Figure 2. Time series of zonal wind anomaly averages (m/s) over (a) the western equatorial Pacific (WEP) and (b) eastern equatorial Pacific (EEP) for the 20CR2 (red line) and ERA20C (blue) data sets. (c and d) As in (a) and (b) but for the 7-year Gaussian low-pass filtered data.

coefficients. Based on the two-tailed Student's t test and the N^{eff} of degrees of freedom defined in equation (4), these two correlation coefficients are statistically significant at the 95% level. Furthermore, these two data sets show an overall strengthening trend of trades in the western equatorial Pacific and an overall weakening trend in the eastern equatorial Pacific (Table 1). In addition, the trends are all statistically significant at the 99% level using the nonparametric Mann-Kendall test (Table 1).

Although there is lower correlation between the two data sets for 7-year Gaussian low-pass-filtered U_{EEP} time series (about 0.69) than U_{WEP} time series (about 0.83), these correlation coefficients are all significant at the 95% confidence level. The result is consistent with that of raw time series. In particular, the trends of the low-pass filtered time series of U_{WEP} and U_{EEP} are almost the same as those of the raw trends and they are all significant at the 99% level (Table 1). Overall, the long-term trend of the trade winds in the equatorial Pacific is inhomogeneous, with a strengthening trend in the western equatorial Pacific and a weakening trend in the eastern equatorial Pacific. These interesting results motivate us to study the causes of this long-term trend of the trades.

3.2. Contribution of ENSO and EM to the Long-Term Trend of the Trades

The tropical Pacific manifests the most important natural climate mode, the El Niño/Southern Oscillation (ENSO). Previous studies have pointed out that its warm (El Niño) phase is stronger and more frequent than its cold (La Niña) phase (e.g., An & Jin, 2004; Jin et al., 2003; Timmermann et al., 1999; Trenberth, 1997; Trenberth & Hoar, 1996). This suggests that ENSO may modulate the long-term trend of the trade winds. Meanwhile, Compo and Sardeshmukh (2010) emphasized that ENSO can be considered as a noise for the long-term trend of global SSTA, and that it probably hinders our understanding of the long-term trend in the tropical Pacific. Based on these points, we want to study whether ENSO can affect the trend of the Pacific trades. To further clarify the possible impact of ENSO, the ENSO signal is first removed and trend analysis is then performed over the tropical Pacific. Specifically, to remove the ENSO signal, the zonal wind anomalies regressed onto the monthly Niño 3 index and the result is then subtracted from the total zonal wind anomalies. Note that it is a challenge to completely remove the variations related to a specific variable from the climate records because of ambiguities arising from nonlinear influences. Although linear regression is one of the most common approaches used to remove the variations associated

Table 1
The 100-Year Trends of the Equatorial Pacific Zonal Wind Anomalies (m/s) for the Raw and 7-Year Gaussian Low-Pass Filtered Time Series of Two Areas: the Western Equatorial Pacific (WEP; 5°S–5°N, 120°E–170°W) and the Eastern Equatorial Pacific (EEP; 5°S–5°N, 150–80°W)[a]

	Original time series		7-year Gaussian low-pass filter time series	
Data Set	WEP	EEP	WEP	EEP
20CR2	−1.40	0.50	−1.40	0.60
ERA-20C	−0.60	0.90	−0.60	0.90

[a]All values are statistically significant at the 99% level (nonparametric Mann-Kendall test).

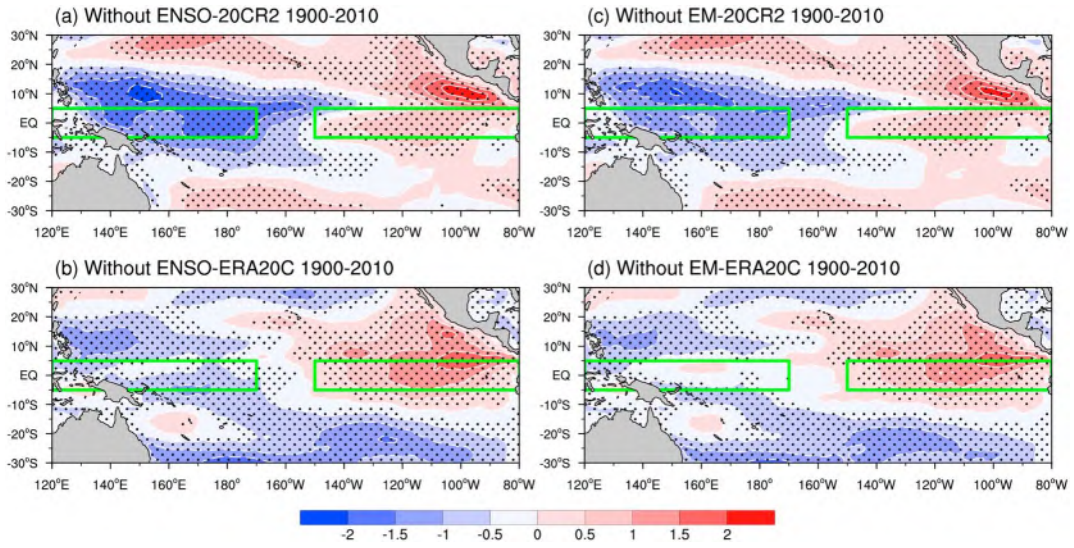

Figure 3. Same as Figure 1 but after removal of the (a and b) El Niño–Southern Oscillation (ENSO) signal and (c and d) El Niño Modoki (EM) signal.

with a specific variable, it only excludes linear components and may not completely exclude the signal in the presence of nonlinear effects (e.g., Zheng et al., 2015; Zheng et al., 2015; Zheng et al., 2017).

Figures 3a and 3b show the long-term trend of trade winds without the ENSO signal over the tropical Pacific. Qualitatively, the long-term trend of trade winds without the ENSO signal (Figures 3a and 3b) is similar to that of the raw trade winds (Figures 1a and 1b) in the two data sets. Namely, there is an overall strengthening trend of trades in the western equatorial Pacific and overall weakening trend in the eastern equatorial Pacific. To reveal the impacts of ENSO on the long-term trend of trade winds more clearly, in the following the long-term trends of the raw U_{WEP} and U_{EEP} are quantitatively compared with those of U_{WEP} and U_{EEP} with the ENSO signal removed. As shown in Figure 6, the long-term trends of U_{WEP} and U_{EEP} without the ENSO signal are roughly consistent with those of the raw U_{WEP} and U_{EEP}. Note that the above results associated with removal of ENSO signal by using Niño 3 index (Figures 3a and 3b and 6) are consistent with that by using Niño 3.4 index (not shown). This suggests that ENSO is not the main driver of the long-term trend of trade winds.

Having shown that ENSO with the most prominent interannual variability does not affect the long-term trend of trade winds over the tropical Pacific, another interannual phenomenon (i.e., EM) is investigated. Figures 3c and 3d show the long-term trend of trade winds without the EM signal over the tropical Pacific. On the whole, Figures 3c and 3d show strengthening of the trade winds over the western equatorial Pacific and weakening of the trade winds over the eastern equatorial Pacific. This is similar to the raw trends (Figures 1a and 1b) and the trends without the ENSO signal (Figures 3a and 3b). However, the trends without the EM signal are weaker than the raw trends in the equatorial Pacific (Figure 6), suggesting that EM has some effect on the long-term trend of trade winds in the equatorial Pacific. This may be related to the modulation of the tropical Pacific mean state by the greater occurrence of EM events (e.g., McPhaden et al., 2011). However, much debate remains about the relationship and interaction between the recent higher occurrence of EM events and the tropical Pacific mean state under global warming (e.g., Lemmon & Karnauskas, 2018, Li et al., 2017, McPhaden et al., 2011, Yeh et al., 2009).

3.3. Contribution of IPO and Global Warming to the Long-Term Trend of Trades

Aside from the interannual variability, IPO and global warming may also contribute to the long-term trend of trade winds in the equatorial Pacific. The first focus is the impacts of IPO on the long-term trend of trades. Figures 4a and 4b show the long-term trend of trade winds without the IPO signal in the tropical Pacific. This long-term trend pattern (Figures 4a and 4b) is similar to the raw trend pattern (Figures 1a and 1b) in the two data sets. Interestingly, the trends without the IPO signal are also weaker than the raw trends in the

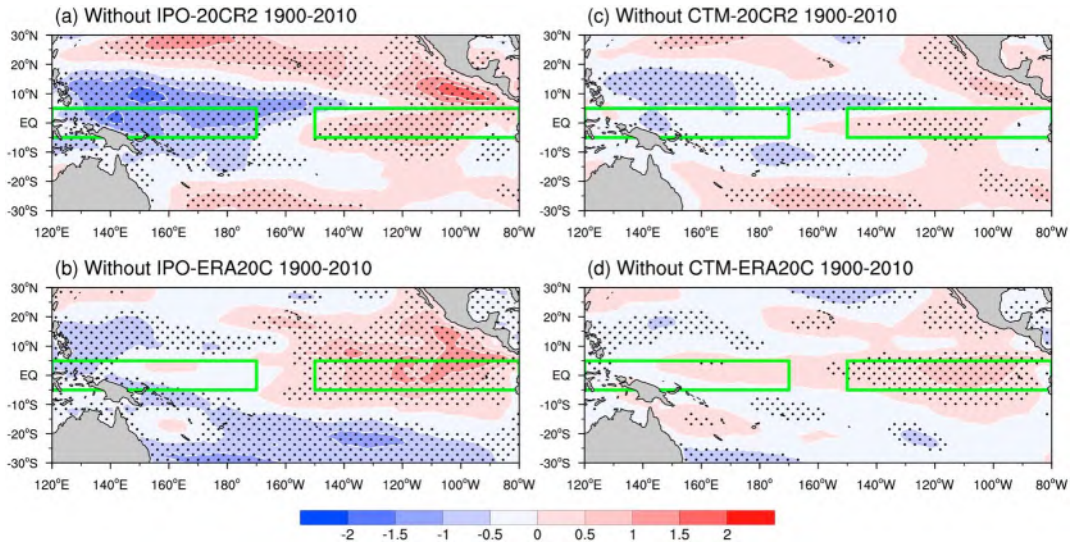

Figure 4. Same as Figure 1 but after removal of the (a and b) Interdecadal Pacific Oscillation (IPO) signal and (c and d) cold tongue mode (CTM) signal.

equatorial Pacific (Figure 6). This means that the IPO may contribute to the long-term trend of trade winds in the equatorial Pacific, which is consistent with other studies (e.g., Dong & Zhou, 2014). However, the IPO can explain only a part of the long-term trend of trades in the equatorial Pacific. In particular for the eastern equatorial Pacific, the long-term trend of U_{EEP} without the IPO signal is roughly close to, although weaker, than that of the raw U_{EEP} in the two data sets (Figures 6b and 6d).

In addition, previous studies have pointed out that global warming plays an important role in the long-term trend of tropical Pacific SST through oceanic dynamical process and thus impacts the long-term trend of the trades (e.g., Cane et al., 1997; Karnauskas et al., 2009; Zhang et al., 2010; Li et al., 2015, 2017; Lemmon & Karnauskas, 2018). Zhang et al. (2010) performed empirical orthogonal function (EOF) analysis of SSTA in the tropical Pacific using multiple SST data sets. The first two modes account for 41.5% and 11.7% of the total variance, respectively (Figure 5). The first EOF mode represents the ENSO variability, with the maximum SSTA in the eastern tropical Pacific. The second EOF mode is identified as a cold tongue mode (hereafter CTM; Figure 5; Lemmon & Karnauskas, 2018; Li et al., 2013; Li et al., 2015, 2017; Zhang et al., 2010). Note that the CTM is independent of the IPO, with completely different spatial and temporal characteristics, as well as a different physical mechanism (Li et al., 2017). Although the increased occurrence of EM event can produce a cooling in the eastern equatorial Pacific, its contribution to the CTM may not be dominant. Because when we remove the EM signal and then perform EOF analysis over the tropical Pacific, the obtained CTM (not shown) is essentially same as raw CTM (Figure 5). The CTM depicts a dipole relationship of SSTA variability between the Pacific cold tongue region and elsewhere in the tropical Pacific (Li et al., 2015, 2017; Li, Sun, & Jin, 2013; Zhang et al., 2010). The positive CTM is characterized by cold SSTA in the Pacific cold tongue region and warm SSTA in the rest of the tropical Pacific. Furthermore, the normalized principal component time series (NPC2) of the CTM exhibits a strong long-term trend (Figure 5). Particularly, the ocean dynamical process makes a major contribution to the long-term trend of the CTM in the tropical Pacific, where vigorous upwelling of cold water in the eastern equatorial region causes weaker warming in the eastern Pacific than in the western Pacific (e.g., Cane et al., 1997; Clement et al., 1996; Karnauskas et al., 2009; Lemmon & Karnauskas, 2018; Li et al., 2015, 2017; Seager & Murtugudde, 1997; Sun & Liu, 1996; Zhang et al., 2010). Since the CTM represents well the long-term trend of the tropical Pacific under global warming (Zhang et al., 2010; Li et al., 2015, 2017; Lemmon & Karnauskas, 2018), the long-term trend of the trade winds is expected to be modified by the CTM.

Figures 4c and 4d show the long-term trend of trade winds without the CTM signal over the tropical Pacific, which differs from the raw trend pattern (Figures 1a and 1b) in the two data sets. Compared with the raw trend (Figures 1a and 1b), the primary difference is that the strengthening trend in the west and the

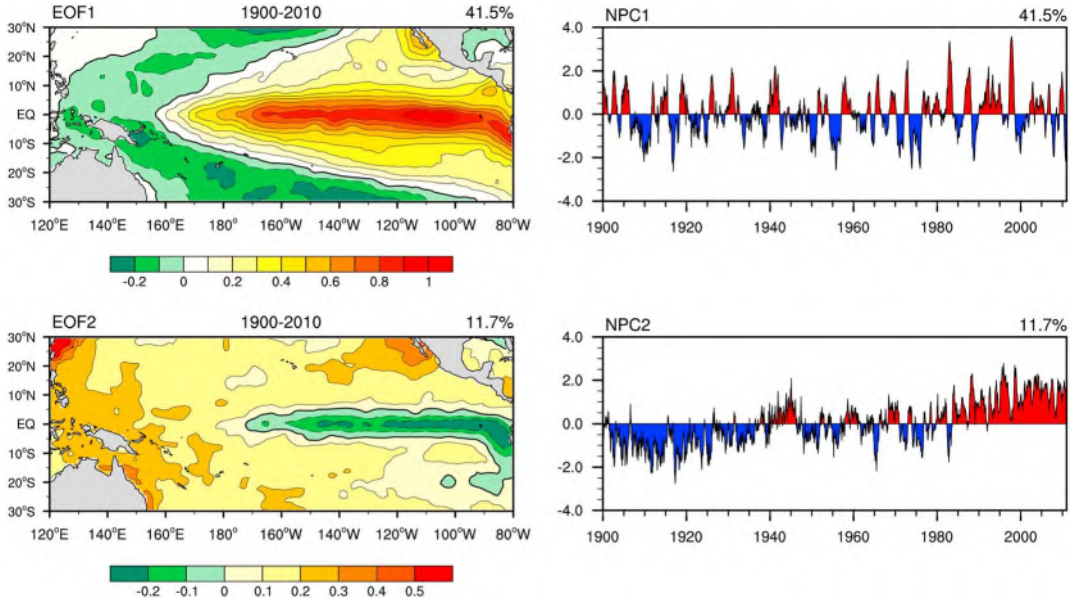

Figure 5. Spatial patterns and corresponding normalized principal components (PCs) of the first two leading empirical orthogonal function (EOF) modes of the tropical Pacific sea surface temperature (SST) anomalies for the HadISST1 data set during 1900–2010.

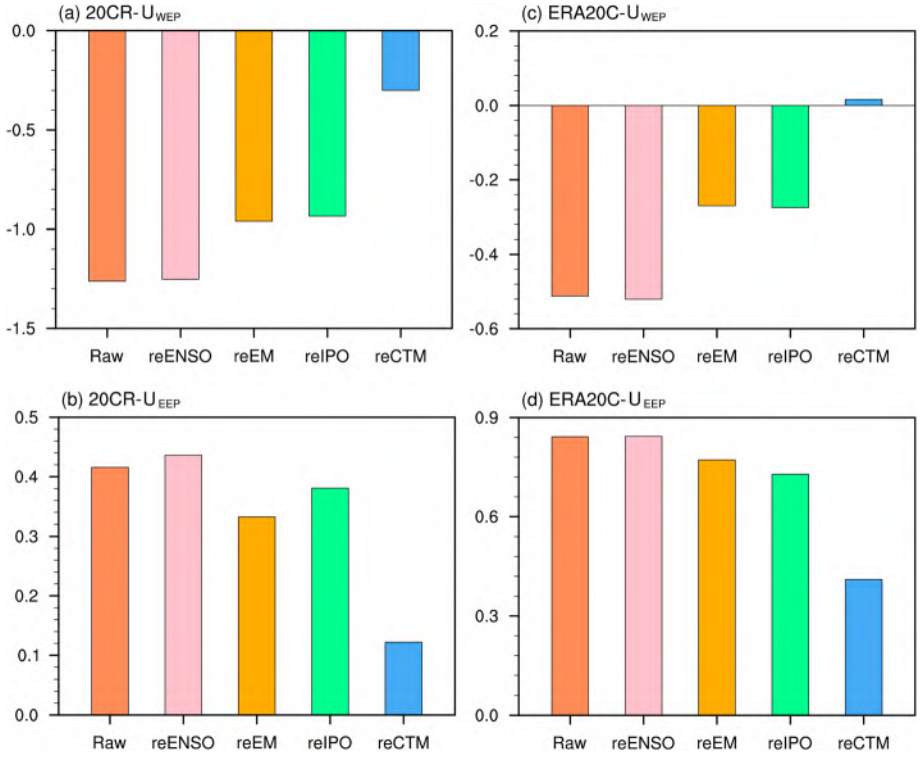

Figure 6. Histograms of the area average values of trends (in m/s per 100 years) of the tropical Pacific zonal wind anomalies over (a) the western equatorial Pacific (WEP) and (b) eastern equatorial Pacific (EEP) for raw (light red) data, and after removing the El Niño–Southern Oscillation (ENSO) signal (pink), El Niño Modoki (EM) signal (orange), Interdecadal Pacific Oscillation (IPO) signal (green), and cold tongue mode (CTM) signal (blue) in the 20CR2 data set. (c and d) As in (a) and (b) but for the ERA20C data set.

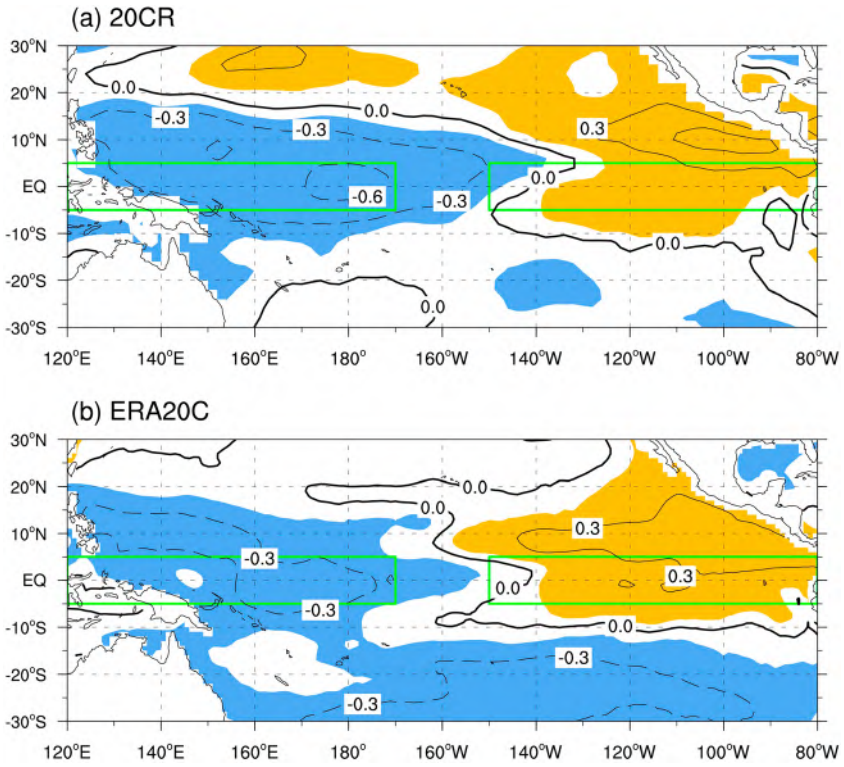

Figure 7. Tropical Pacific zonal wind anomalies (m/s) in the (a) 20CR2 data set regressed upon the NPC2 time series over 1900–2010. Shading indicates the correlation coefficients exceed the 99% confidence level. (b) As in (a) but for the ERA20C data set. The two green boxes are same as Figure 1.

weakening trend in the east are weak in the two data sets (Figures 4c and 4d). Especially for the EAR20C data set, the trade winds in the western equatorial Pacific have a weakening trend (Figure 4d). These results are also confirmed in Figure 6. As shown in Figure 6, the trends in the equatorial Pacific without the CTM signal are the weakest of the raw trends and the trends after removal of the ENSO, EM, and IPO signals. Note that if the global warming signal is represented by the HadCRUT4 global mean surface temperature (e.g., Li et al., 2015, Zhang et al., 2010), the trends without the global warming signal are also weaker than the raw trends and the trends with the ENSO, EM, and IPO signals removed (not shown). It is suggested that the CTM under global warming is predominantly responsible for the long-term trend of the trade winds in the equatorial Pacific. This begs a question: What is the mechanism for the impact of the CTM on the long-term trend of the trades under global warming?

3.4. Possible Mechanism Responsible for the Long-Term Trend of the Trades Under Global Warming

Figure 7 shows the tropical Pacific zonal wind anomalies regressed upon the NPC2 time series of the CTM in the two data sets. Interestingly, both regressed patterns correspond to strengthening trades in the western equatorial Pacific and weakening trades in the eastern equatorial Pacific (Figure 7). This result is consistent with the results of Zhang et al. (2010) and Li et al. (2015), who showed La Niña-like patterns of atmospheric wind anomalies associated with the positive CTM. Because the CTM has a strong long-term trend, it is suggested that the long-term trend of the CTM could modify the long-term trend of the trade winds. This can be partly explained by the Gill–Matsuno mechanism as a response of the atmosphere to equatorial thermal forcing (e.g., Gill, 1980, Matsuno, 1966). Based on the Gill-Matsuno mechanism, if the cooling SSTA associated with the CTM appears in the eastern equatorial Pacific, the Rossby wave and Kelvin wave responses correspond to the easterly and westerly winds, respectively. Similarly, when the warming SSTA related to the CTM is set in the western equatorial Pacific, the Rossby wave and Kelvin wave responses correspond to the westerly and easterly winds, respectively. This means that the strengthening trend of the trades in the

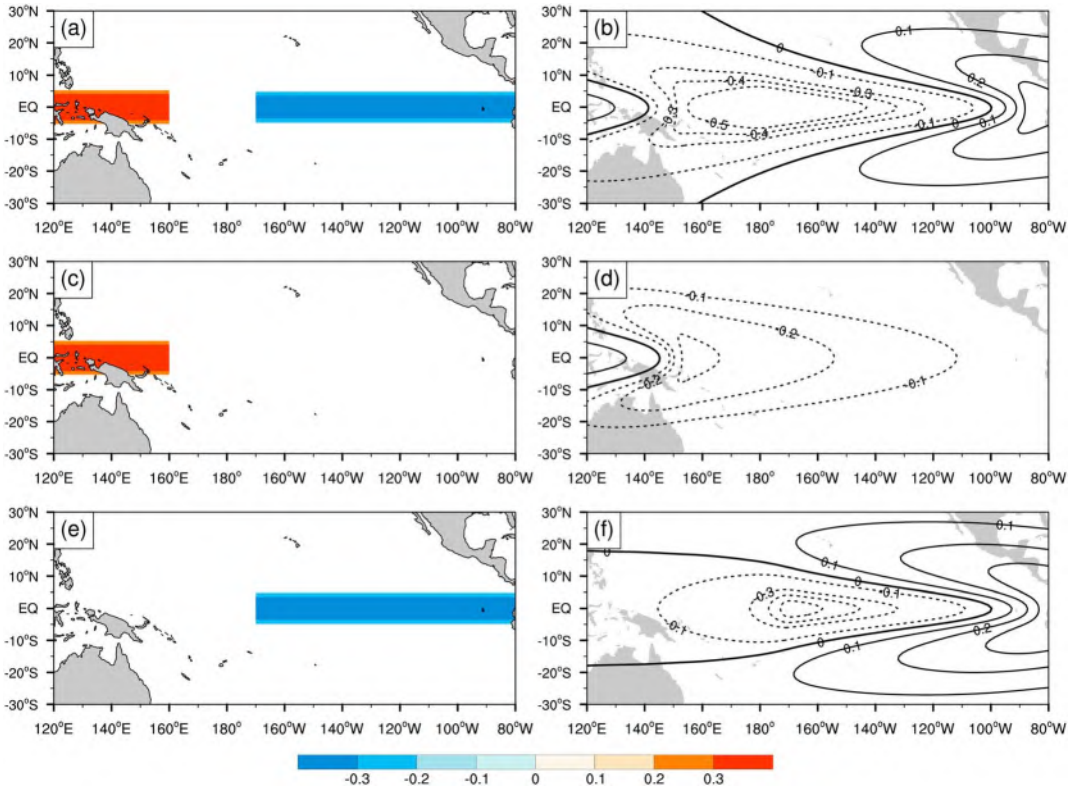

Figure 8. (a) Distribution of the initial ideal heating source over the western equatorial Pacific and cooling source over the eastern equatorial Pacific for the Gill model. (b) Zonal winds in the lower layer for the heating dipole shown in (a). (c and e) As in (a) and (d and f) as in (b) but for the heating source over the western equatorial Pacific and cooling source over the eastern equatorial Pacific, respectively.

western equatorial Pacific and weakening trend in the eastern equatorial Pacific are all modified by the long-term trend of the CTM through the Gill–Matsuno mechanism.

To confirm the role of SSTA trend associated with the CTM on long-term changes in the trades of the equatorial Pacific, a simple analytic model (i.e., the Gill model; e.g., Gill, 1980; Matsuno, 1966; Xing et al., 2014, 2016; Zhang et al., 2018) is used in the present study. Since the zonal SST gradient over the equatorial Pacific is crucial in determining the trends of Walker circulation and trades (e.g., Meng et al., 2012, Sandeep et al., 2014), the distribution of warming and cooling SSTA associated with the CTM over the equatorial Pacific is expected to play an important role in the trades trend.

Figure 8a shows the distribution of the initial ideal heating source over the western equatorial Pacific and cooling source over the eastern equatorial Pacific for the Gill model. Note that the zonal width of cooling source is wider than that of heating source, but the intensity of cooling source is weaker than that of heating source (Figure 8a). This is consistent with the equatorial Pacific SSTA associated with the positive CTM (Figure 5). Analytical solutions to the forcing are given in Figure 8b. In addition to the westerly winds in the equatorial Pacific west of 140°E, there are overall easterly winds in the western equatorial Pacific and westerly winds in the eastern equatorial Pacific (Figure 8b). This result is consistent with the observational long-term trend of the trades (Figure 1) and the trades related to the CTM (Figure 7), except for the observational strengthening trades in the equatorial Pacific west of 140°E (Figure 1), which may be associated with tropical interbasin SST gradient (Zhang & Karnauskas, 2016) or other factors. Overall, these results mentioned above suggest that the heating dipole sources associated with the CTM play an important role in the long-term trend of equatorial Pacific trades.

According to the Gill-Matsuno theory, the Rossby and Kelvin waves forced by the equatorial heating and cooling sources give wind fields in Figure 8b. Thus, are the wind responses similar to the observational trades trend (Figure 1) if only considering the isolated heating source or cooling source? To address this question, we first take the isolated heating source in the western equatorial Pacific into consideration

(Figure 8c), and the atmospheric responses of the wind fields to the heating source are displayed in Figure 8 d. It is clear that the Rossby and Kelvin waves forced by the equatorial hearing source give westerly winds in the equatorial Pacific west of 140°E and easterly winds in the western equatorial Pacific (Figure 8d), respectively. This indicates that the equatorial heating source associated with the CTM makes a contribution to the strengthening trend of the trades in the western equatorial Pacific. However, the lack of the westerly winds in the eastern equatorial Pacific (Figure 8d) is not consistent with the observations (Figure 1). This suggests that it is not enough to consider only the isolated heating source. Similarly, if the isolated cooling source builds in the eastern equatorial Pacific (Figure 8e), one can be seen in Figure 8f that the Rossby and Kelvin waves forced by the equatorial cooling source give easterly winds in the western equatorial Pacific and westerly winds in the eastern equatorial Pacific. This result is also consistent with the long-term trend of the trades (Figure 1) and the trades related to the CTM (Figure 7), indicating that the isolated cooling source in the eastern equatorial Pacific plays an important role in the long-term trend of Pacific trades. In short, the cooling source associated with the CTM contributes to the strengthening trend of the trades in the western equatorial Pacific and weakening trend in the eastern equatorial Pacific, and the heating source associated with the CTM only contributes to the strengthening trades in the western equatorial Pacific. This indicates that the cooling and warming SSTA associated with the CTM in the equatorial Pacific together induce the observational trends of Pacific trades (Figure 1) through the Gill-Matsuno theory.

Note that the Gill-Matsuno theory explains a part of the long-term trend of trades along the equatorial Pacific, but not all. This is because the typical Gill pattern is generated as a result of the linear response of the model atmosphere, whose basic state is assumed to be at rest (e.g., Guan et al., 2003). However, the real atmosphere is complex with nonlinear physical processes. Probably for this reason, the dividing line between easterly and westerly winds (Figure 8b) is farther east than in the observations (Figure 1) over the equatorial Pacific. Despite the crudeness of this numerical simulation, which lacks the impacts of other factors on tropical Pacific trades, the general similarity with observations lends support to the idea that the long-term trend of SSTA associated with the CTM can give the strengthening trend of trades in the western equatorial Pacific and weakening trend in the eastern equatorial Pacific.

4. Discussion and Conclusions

The long-term trend of trade winds in the tropical Pacific was investigated using two different data sets (20CR2 and ERA20C). There is a strengthening trend of the trades in the western equatorial Pacific and a weakening trend in the eastern equatorial Pacific (Figures 1 and 2). Note that several factors may influence the long-term trend of trades along the equatorial Pacific. Of the two important interannual modes, ENSO does not greatly affect the long-term trend of trade winds, while the EM has some impact on their long-term trend. The more frequent occurrences of the EM under global warming may affect the long-term trend in the Pacific trades (e.g., Sohn et al., 2013).

The interdecadal mode, the IPO, can only explain a part of the long-term trend of trades in the equatorial Pacific, particularly for the eastern equatorial Pacific (Figure 6). The major part of the long-term trend of the trades along the equatorial Pacific is contributed by the CTM. The long-term trend of tropical Pacific SSTA associated with the CTM is induced by ocean dynamical feedback under the forcing of global warming. According to the Gill-Matsuno mechanism, the equatorial Pacific cooling and warming SSTA associated with the CTM together induce easterly winds over the western equatorial Pacific, while the eastern equatorial Pacific cooling SSTA associated with the CTM also induces westerly winds over the eastern equatorial Pacific. Although there are some feedback between the CTM and trade winds, these feedback make a minor contribution to the CTM in comparison with the ocean dynamical feedback under global warming (Li et al., 2015). It is also noted that the tropical Pacific SST will tend to warm in the initial period of global warming, which may induce a weakening Walker circulation through a response of different increasing rates for water vapor and precipitation to global warming (Held & Soden, 2006; Vecchi et al., 2006). However, the strong upwelling in the eastern equatorial Pacific could bring up colder waters to reverse the initial warming. Therefore, the long-term change of tropical Pacific SSTA displays the CTM pattern under global warming (Li et al., 2015, 2017), which contributes to the long-term trend of tropical Pacific trades. Overall, the CTM plays a dominant role in the long-term trend of equatorial Pacific trades compared with ENSO, EM,

and IPO. Except for these factors mentioned above, note that the centennial-scale variability (Giese & Ray, 2011; Ray & Giese, 2012) and tropical interbasin SST gradient (Zhang & Karnauskas, 2016) may also contribute to the trades trend.

In addition, Wang et al. (2012) pointed out that the enhanced trades in the tropical Pacific might transport and converge moisture into the Eastern Hemisphere monsoon regions, thereby leading to a *wet-gets-wetter* and *dry-gets-drier* trend pattern in global precipitation. This suggests that the CTM may affect the long-term trend of global precipitation through modifying the long-term trend of the trades. In future work, it is intended to carry out further research into the impacts of the CTM on the long-term trend of global precipitation under global warming, and this should give a clearer understanding of the physical mechanism associated with the impacts of global warming on global precipitation.

Acknowledgments
We thank Kristopher Karnauskas for constructive comments and suggestions. We also acknowledge the helpful suggestions and comments of two anonymous reviewers. This work was jointly supported by the National Key Research and Development Program on Monitoring, Early Warning and Prevention of Major Natural Disaster (2018YFC1506006), National Natural Science Foundation of China Project (41805054, 41875108, 41805041, and 41705050), SOA International Cooperation Program on Global Change and Air-Sea Interactions (GASI-IPOVAI-03), and National Key R&D Program of China (2016YFA0601801). The ERA20C data set was obtained from the European Centre for Medium-Range Weather Forecasts (ECMWF) and can be downloaded from http://apps.ecmwf.int/datasets/data/era20c-moda/levtype=sfc/type=an/. The 20CR2 data set was obtained from the National Oceanic and Atmospheric Administration (NOAA) and is available at http://www.esrl.noaa.gov/psd/data/gridded/data.20thC_ReanV2.monolevel.mm.html. The HadISST1 and HadCRUT4 datasets were obtained from the UK Met Office Hadley Centre and can be downloaded from http://www.metoffice.gov.uk/hadobs/hadisst/data/download.html and http://www.cru.uea.ac.uk/cru/data/temperature/, respectively.

References

An, S. I., & Jin, F. F. (2004). Nonlinearity and asymmetry of ENSO. *Journal of Climate*, *17*(12), 2399–2412. https://doi.org/10.1175/1520-0442(2004)017<2399:NAAOE>2.0.CO;2

Ashok, K., Behera, S. K., Rao, S. A., Weng, H. Y., & Yamagata, T. (2007). El Niño Modoki and its possible teleconnection. *Journal of Geophysical Research*, *112*, C11007. https://doi.org/10.1029/2006JC003798

Balmaseda, M. A., Trenberth, K. E., & Kallen, E. (2013). Distinctive climate signals in reanalysis of global ocean heat content. *Geophysical Research Letters*, *40*, 1754–1759. https://doi.org/10.1002/grl.50382

Battisti, D. S., & Hirst, A. C. (1989). Interannual variability in a tropical atmosphere-ocean model: Influence of the basic state, ocean geometry and nonlinearity. *Journal of the Atmospheric Sciences*, *46*(12), 1687–1712. https://doi.org/10.1175/1520-0469(1989)046<1687:IVIATA>2.0.CO;2

Bjerknes, J. (1969). Atmospheric teleconnections from equatorial Pacific. *Monthly Weather Review*, *97*(3), 163–172. https://doi.org/10.1175/1520-0493(1969)097<0163:ATFTEP>2.3.CO;2

Boisséson, E., Balmaseda, M., Abdalla, S., Källén, E., & Janssen, P. (2014). How robust is the recent strengthening of the tropical Pacific trade winds? *Geophysical Research Letters*, *41*, 4398–4405. https://doi.org/10.1002/2014GL060257

Bretherton, C. S., Widmann, M., Dymnikov, V. P., Wallace, J. M., & Blade, I. (1999). The effective number of spatial degrees of freedom of a time-varying field. *Journal of Climate*, *12*(7), 1990–2009. https://doi.org/10.1175/1520-0442(1999)012<1990:TENOSD>2.0.CO;2

Cane, M. A., Clement, A. C., Kaplan, A., Kushnir, Y., Pozdnyakov, D., Seager, R., et al. (1997). Twentieth-century sea surface temperature trends. *Science*, *275*(5302), 957–960. https://doi.org/10.1126/science.275.5302.957

Chen, D. K., Lian, T., Fu, C. B., Cane, M. A., Tang, Y. M., Murtugudde, R., et al. (2015). Strong influence of westerly wind bursts on El Niño diversity. *Nature Geoscience*, *8*(5), 339–345. https://doi.org/10.1038/ngeo2399

Clement, A. C., Seager, R., Cane, M. A., & Zebiak, S. E. (1996). An ocean dynamical thermostat. *Journal of Climate*, *9*(9), 2190–2196. https://doi.org/10.1175/1520-0442(1996)009<2190:AODT>2.0.CO;2

Coats, S., & Karnauskas, K. B. (2017). Are simulated and observed twentieth century tropical Pacific sea surface temperature trends significant relative to internal variability? *Geophysical Research Letters*, *44*, 9928–9937. https://doi.org/10.1002/2017GL074622

Collins, M., An, S. I., Cai, W. J., Ganachaud, A., Guilyardi, E., Jin, F. F., et al. (2010). The impact of global warming on the tropical Pacific Ocean and El Niño. *Nature Geoscience*, *3*(6), 391–397. https://doi.org/10.1038/ngeo868

Compo, G. P., & Sardeshmukh, P. D. (2010). Removing ENSO-related variations from the climate record. *Journal of Climate*, *23*(8), 1957–1978. https://doi.org/10.1175/2009JCLI2735.1

Compo, G. P., Whitaker, J. S., Sardeshmukh, P. D., Matsui, N., Allan, R. J., Yin, X., et al. (2011). The twentieth century reanalysis project. *Quarterly Journal of the Royal Meteorological Society*, *137*(654), 1–28. https://doi.org/10.1002/qj.776

DiNezio, P. N., Clement, A. C., Vecchi, G. A., Soden, B. J., & Kirtman, B. P. (2009). Climate response of the equatorial Pacific to global warming. *Journal of Climate*, *22*(18), 4873–4892. https://doi.org/10.1175/2009JCLI2982.1

Ding, R. Q., Li, J. P., & Tseng, Y. H. (2015). The impact of South Pacific extratropical forcing on ENSO and comparisons with the North Pacific. *Climate Dynamics*, *44*(7-8), 2017–2034. https://doi.org/10.1007/s00382-014-2303-5

Ding, R. Q., Li, J. P., Tseng, Y. H., Sun, C., & Guo, Y. P. (2015). The Victoria mode in the North Pacific linking extratropical sea level pressure variations to ENSO. *Journal of Geophysical Research: Atmospheres*, *120*, 27–45. https://doi.org/10.1002/2014JD022221

Dong, L., & Zhou, T. J. (2014). The formation of the recent cooling in the eastern tropical Pacific Ocean and the associated climate impacts: A competition of global warming, IPO, and AMO. *Journal of Geophysical Research: Atmosphere*, *119*, 11,272–11,287. https://doi.org/10.1002/2013JD021395

Drenkard, E. J., & Karnauskas, K. B. (2014). Strengthening of the Pacific equatorial undercurrent in the SODA reanalysis: Mechanisms, ocean dynamics, and implications. *Journal of Climate*, *27*(6), 2405–2416. https://doi.org/10.1175/JCLI-D-13-00359.1

England, M. H., McGregor, S., Spence, P., Meehl, G. A., Timmermann, A., Cai, W. J., et al. (2014). Recent intensification of wind-driven circulation in the Pacific and the ongoing warming hiatus. *Nature Climate Change*, *4*(3), 222–227. https://doi.org/10.1038/nclimate2106

Feng, J., & Li, J. P. (2011). Influence of El Niño Modoki on spring rainfall over south China. *Journal of Geophysical Research*, *116*, D13102. https://doi.org/10.1029/2010JD015160

Feng, J., & Li, J. P. (2013). Contrasting impacts of two types of ENSO on the boreal spring Hadley circulation. *Journal of Climate*, *26*(13), 4773–4789. https://doi.org/10.1175/JCLI-D-12-00298.1

Funk, C. C., & Hoell, A. (2015). The leading mode of observed and CMIP5 ENSO-residual sea surface temperatures and associated changes in Indo-Pacific climate. *Journal of Climate*, *28*(11), 4309–4329. https://doi.org/10.1175/JCLI-D-14-00334.1

Giese, B. S., & Ray, S. (2011). El Niño variability in simple ocean data assimilation (SODA), 1871–2008. *Journal of Geophysical Research*, *116*, C02024. https://doi.org/10.1029/2010JC006695

Gill, A. (1980). Some simple solutions for heat-induced tropical circulation. *Quarterly Journal of the Royal Meteorological Society*, *106*(449), 447–462. https://doi.org/10.1002/qj.49710644905

Guan, Z., Ashok, K., & Yamagata, T. (2003). Summertime response of the tropical Atmosphere to the Indian Ocean dipole sea surface temperature anomalies. *Journal of the Meteorological Society of Japan*, *81*(3), 533–561. https://doi.org/10.2151/jmsj.81.533

Held, I. M., & Soden, B. J. (2006). Robust responses of the hydrological cycle to global warming. *Journal of Climate*, *19*(21), 5686–5699. https://doi.org/10.1175/JCLI3990.1

Henley, B. J., Gergis, J., Karoly, D. J., Power, S., Kennedy, J., & Folland, C. K. (2015). A tripole index for the interdecadal Pacific oscillation. *Climate Dynamics*, *45*(11-12), 3077–3090. https://doi.org/10.1007/s00382-015-2525-1

Jin, F. F. (1997a). An equatorial ocean recharge paradigm for ENSO. Part1: Conceptual model. *Journal of the Atmospheric Sciences*, *54*(7), 811–829. https://doi.org/10.1175/1520-0469(1997)054<0811:AEORPF>2.0.CO;2

Jin, F. F. (1997b). An equatorial ocean recharge paradigm for ENSO. Part2: A stripped-down coupled model. *Journal of the Atmospheric Sciences*, *54*(7), 830–847. https://doi.org/10.1175/1520-0469(1997)054<0830:AEORPF>2.0.CO;2

Jin, F. F., An, S. I., Timmermann, A., & Zhao, J. (2003). Strong El Niño events and nonlinear dynamical heating. *Geophysical Research Letters*, *30*(3), 1120. https://doi.org/10.1029/2002GL016356

Kao, H. Y., & Yu, J. Y. (2009). Contrasting eastern-Pacific and central-Pacific types of ENSO. *Journal of Climate*, *22*(3), 615–632. https://doi.org/10.1175/2008JCLI2309.1

Karnauskas, K. B. (2013). Can we distinguish canonical El Niño from Modoki? *Geophysical Research Letters*, *40*, 5246–5251. https://doi.org/10.1002/grl.51007

Karnauskas, K. B., Seager, R., Kaplan, A., Kushnir, Y., & Cane, M. A. (2009). Observed strengthening of the zonal sea surface temperature gradient across the equatorial Pacific Ocean. *Journal of Climate*, *22*(16), 4316–4321. https://doi.org/10.1175/2009JCLI2936.1

Kosaka, Y., & Xie, S. P. (2013). Recent global-warming hiatus tied to equatorial Pacific surface cooling. *Nature*, *501*(7467), 403–407. https://doi.org/10.1038/nature12534

Kug, J. S., Jin, F. F., & An, S. I. (2009). Two types of El Niño events: Cold tongue El Niño and warm pool El Niño. *Journal of Climate*, *22*(6), 1499–1515. https://doi.org/10.1175/2008JCLI2624.1

Larkin, N. K., & Harrison, D. E. (2005). On the definition of El Niño and associated seasonal average US weather anomalies. *Geophysical Research Letters*, *32*, L13705. https://doi.org/10.1029/2005GL022738

Lemmon, D. E., & Karnauskas, K. B. (2018). A metric for quantifying El Niño pattern diversity with implications for ENSO–mean state interaction. *Climate Dynamics*. https://doi.org/10.1007/s00382-018-4194-3

L'Heureux, M. L., Lee, S., & Lyon, B. (2013). Recent multidecadal strengthening of the Walker circulation across the tropical Pacific. *Nature Climate Change*, *3*(6), 571–576. https://doi.org/10.1038/nclimate1840

Li, G., & Ren, B. H. (2012). Evidence for strengthening of the tropical Pacific Ocean surface wind speed during 1979–2001. *Theoretical and Applied Climatology*, *107*(1–2), 59–72. https://doi.org/10.1007/s00704-011-0463-3

Li, J., Feng, J., & Li, Y. (2011). A possible cause of decreasing summer rainfall in northeast Australia. *International Journal of Climatology*, *32*(7), 995–1005. https://doi.org/10.1002/joc.2328

Li, J. P., Ren, R. C., Qi, Y. Q., Wang, F. M., Lu, R. Y., Zhang, P. Q., et al. (2013). Progress in air-land-sea interactions in Asia and their role in global and Asian climate change (in Chinese). *Chinese Journal of Atmospheric Sciences*, *37*(2), 518–538.

Li, J. P., Sun, C., & Jin, F. F. (2013). NAO implicated as a predictor of Northern Hemisphere mean temperature multidecadal variability. *Geophysical Research Letters*, *40*, 5497–5502. https://doi.org/10.1002/2013GL057877

Li, J. P., & Zhang, L. (2008). Wind onset and withdrawal of Asian summer monsoon and their simulated performance in AMIP models. *Climate Dynamics*, *32*(7-8), 935–968. https://doi.org/10.1007/s00382-008-0465-8

Li, Y., Li, J. P., & Feng, J. (2012). A teleconnection between the reduction of rainfall in southwest Western Australia and North China. *Journal of Climate*, *25*(24), 8444–8461. https://doi.org/10.1175/JCLI-D-11-00613.1

Li, Y., Li, J. P., Zhang, W. J., Chen, Q. L., Feng, J., Zheng, F., et al. (2017). Impacts of the tropical Pacific cold tongue mode on ENSO diversity under global warming. *Journal of Geophysical Research: Oceans*, *122*, 8524–8542. https://doi.org/10.1002/2017JC013052

Li, Y., Li, J. P., Zhang, W. J., Zhao, X., Xie, F., & Zheng, F. (2015). Ocean dynamical processes associated with the tropical Pacific cold tongue mode. *Journal of Geophysical Research: Oceans*, *120*, 6419–6435. https://doi.org/10.1002/2015JC010814

Lian, T., Chen, D., Tang, Y., & Wu, Q. (2014). Effects of westerly wind bursts on El Niño: A new perspective. *Geophysical Research Letters*, *41*, 3522–3527. https://doi.org/10.1002/2014GL059989

Ma, S. M., & Zhou, T. J. (2016). Robust strengthening and westward shift of the tropical Pacific Walker circulation during 1979–2012: A comparison of 7 sets of reanalysis data and 26 CMIP5 models. *Journal of Climate*, *29*(9), 3097–3118. https://doi.org/10.1175/JCLI-D-15-0398.1

Matsuno, T. (1966). Quasi-geostrophic motions in the equatorial area. *Journal of the Meteorological Society of Japan. Ser. II*, *44*(1), 25–43. https://doi.org/10.2151/jmsj1965.44.1_25

McPhaden, M. J., Lee, T., & McClurg, D. (2011). El Niño and its relationship to changing background conditions in the tropical Pacific Ocean. *Geophysical Research Letters*, *38*, L13705. https://doi.org/10.1029/2011GL048275

Meng, Q., Latif, M., Park, W., Keenlyside, N. S., Semenov, V. A., & Martin, T. (2012). Twentieth century Walker Circulation change: Data analysis and model experiments. *Climate Dynamics*, *38*(9-10), 1757–1773. https://doi.org/10.1007/s00382-011-1047-8

Morice, C. P., Kennedy, J. J., Rayner, N. A., & Jones, P. D. (2012). Quantifying uncertainties in global and regional temperature change using an ensemble of observational estimates: The HadCRUT4 data set. *Journal of Geophysical Research*, *117*, D08101. https://doi.org/10.1029/2011JD017187

Poli, P., Hersbach, H., Dee, D. P., Berrisford, P., Simmons, A. J., Vitart, F., et al. (2016). ERA-20C: An atmospheric reanalysis of the twentieth century. *Journal of Climate*, *29*(11), 4083–4097. https://doi.org/10.1175/JCLI-D-15-0556.1

Ray, S., & Giese, B. S. (2012). Historical changes in El Niño and La Niña characteristics in an ocean reanalysis. *Journal of Geophysical Research*, *117*, C11007. https://doi.org/10.1029/2012JC008031

Rayner, N. A., Parker, D. E., Horton, E. B., Folland, C. K., Alexander, L. V., Rowell, D. P., et al. (2003). Global analyses of sea surface temperature, sea ice, and night marine air temperature since the late nineteenth century. *Journal of Geophysical Research*, *108*(D14), 4407. https://doi.org/10.1029/2002JD002670

Ren, H. L., & Jin, F. F. (2011). Niño indices for two types of ENSO. *Geophysical Research Letters*, *38*, L04704. https://doi.org/10.1029/2010GL046031

Ren, H. L., & Jin, F. F. (2013). Recharge oscillator mechanisms in two types of ENSO. *Journal of Climate*, *26*(17), 6506–6523. https://doi.org/10.1175/JCLI-D-12-00601.1

Ren, H. L., Jin, F. F., Stuecker, M. F., & Xie, R. (2013). ENSO regime change since the late 1970s as manifested by two types of ENSO. *Journal of the Meteorological Society of Japan. Ser. II*, *91*(6), 835–842. https://doi.org/10.2151/jmsj.2013-608

Sandeep, S., Stordal, F., Sardeshmukh, P. D., & Compo, G. P. (2014). Pacific Walker Circulation variability in coupled and uncoupled climate models. *Climate Dynamics*, *43*(1-2), 103–117. https://doi.org/10.1007/s00382-014-2135-3

Seager, R., & Murtugudde, R. (1997). Ocean dynamics, thermocline adjustment, and regulation of tropical SST. *Journal of Climate*, *10*(3), 521–534. https://doi.org/10.1175/1520-0442(1997)010<0521:ODTAAR>2.0.CO;2

Sen, P. K. (1968). Estimates of the regression coefficient based on Kendall's Tau. *Journal of the American Statistical Association*, *63*(324), 1379–1389. https://doi.org/10.1080/01621459.1968.10480934

Sohn, B. J., Yeh, S.-W., Schmetz, J., & Song, H.-J. (2013). Observational evidences of Walker circulation change over the last 30 years contrasting with GCM results. *Climate Dynamics*, *40*(7-8), 1721–1732. https://doi.org/10.1007/s00382-012-1484-z

Solomon, A., & Newman, M. (2012). Reconciling disparate twentieth-century Indo-Pacific ocean temperature trends in the instrumental record. *Nature Climate Change*, *2*(9), 691–699. https://doi.org/10.1038/nclimate1591

Suarez, M. J., & Schopf, P. S. (1988). A delayed action oscillator for ENSO. *Journal of the Atmospheric Sciences*, *45*(21), 3283–3287. https://doi.org/10.1175/1520-0469(1988)045<3283:ADAOFE>2.0.CO;2

Sun, D. Z., & Liu, Z. Y. (1996). Dynamic ocean-atmosphere coupling: A thermostat for the tropics. *Science*, *272*(5265), 1148–1150. https://doi.org/10.1126/science.272.5265.1148

Takahashi, C., & Watanabe, M. (2016). Pacific trade winds accelerated by aerosol forcing over the past two decades. *Nature Climate Change*, *6*(8), 768–772. https://doi.org/10.1038/nclimate2996

Takahashi, K., Montecinos, A., Goubanova, K., & Dewitte, B. (2011). ENSO regimes: Reinterpreting the canonical and Modoki El Niño. *Geophysical Research Letters*, *38*, L10704. https://doi.org/10.1029/2011GL047364

Theil, H. (1950). A rank-invariant method of linear and polynomial regression analysis. *Proc. Kon. Ned. Adad. V. Wetensch. A*, *53*, 386–392. 521–525, 1397–1412

Timmermann, A., Oberhuber, J., Bacher, A., Esch, M., Latif, M., & Roeckner, E. (1999). Increased El Niño frequency in a climate model forced by future greenhouse warming. *Nature*, *398*(6729), 694–697. https://doi.org/10.1038/19505

Trenberth, K. E. (1997). The definition of El Niño. *Bulletin of the American Meteorological Society*, *78*(12), 2771–2777. https://doi.org/10.1175/1520-0477(1997)078<2771:TDOENO>2.0.CO;2

Trenberth, K. E., & Fasullo, J. T. (2013). An apparent hiatus in global warming? *Earth's Future*, *1*(1), 19–32. https://doi.org/10.1002/2013EF000165

Trenberth, K. E., & Hoar, T. J. (1996). The 1990–1995 El Niño-Southern Oscillation event: Longest on record. *Geophysical Research Letters*, *23*(1), 57–60. https://doi.org/10.1029/95GL03602

Vecchi, G. A., Clement, A., & Soden, B. J. (2008). Examining the tropical Pacific's response to global warming. *Eos, Transactions American Geophysical Union*, *89*(9), 81–83. https://doi.org/10.1029/2008EO090002

Vecchi, G. A., Soden, B. J., Wittenberg, A. T., Held, I. M., Leetmaa, A., & Harrison, M. J. (2006). Weakening of tropical Pacific atmospheric circulation due to anthropogenic forcing. *Nature*, *441*(7089), 73–76. https://doi.org/10.1038/nature04744

Vera, C., Higgins, W., Amador, J., Ambrizzi, T., Garreaud, R., Gochis, D., et al. (2006). Toward a unified view of the American monsoon systems. *Journal of Climate*, *19*(20), 4977–5000. https://doi.org/10.1175/JCLI3896.1

Wang, B., Liu, J., Kim, H. J., Webster, P. J., & Yim, S. Y. (2012). Recent change of the global monsoon precipitation (1979–2008). *Climate Dynamics*, *39*(5), 1123–1135. https://doi.org/10.1007/s00382-011-1266-z

Xie, F., Li, J. P., Tian, W. S., Fu, Q., Jin, F. F., Hu, Y. Y., et al. (2016). A connection from Arctic stratospheric ozone to El Niño-Southern oscillation. *Environmental Research Letters*, *11*(12), 124026. https://doi.org/10.1088/1748-9326/11/12/124026

Xie, F., Li, J. P., Zhang, J. K., Tian, W. S., Hu, Y. Y., Zhao, S., et al. (2017). Variations in North Pacific sea surface temperature caused by Arctic stratospheric ozone anomalies. *Environmental Research Letters*, *12*(11), 114023. https://doi.org/10.1088/1748-9326/aa9005

Xing, N., Li, J. P., Jiang, X. W., & Wang, L. N. (2016). Local oceanic precursors for the summer monsoon onset over the bay of Bengal and the underlying processes. *Journal of Climate*, *29*(23), 8455–8470. https://doi.org/10.1175/JCLI-D-15-0825.1

Xing, N., Li, J. P., & Li, Y. K. (2014). Response of the tropical atmosphere to isolated equatorially asymmetric heating (in Chinese. *Chinese Journal of Atmospheric Sciences*, *38*(6), 1147–1158.

Yang, C. X., Giese, B. S., & Wu, L. X. (2014). Ocean dynamics and tropical Pacific climate change in ocean reanalyses and coupled climate models. *Journal of Geophysical Research: Oceans*, *119*, 7066–7077. https://doi.org/10.1002/2014JC009979

Yang, R. W., Wang, J., Zhang, T., & He, S. (2017). Change in the relationship between the Australian summer monsoon circulation and boreal summer precipitation over Central China in the late 1990s. *Meteorology and Atmospheric Physics*, *131*(1), 105–113. https://doi.org/10.1007/s00703-017-0556-3

Yang, R. W., Xie, Z., & Cao, J. (2017). A dynamic index for the westward ridge point variability of the Western Pacific subtropical high during summer. *Journal of Climate*, *30*(9), 3325–3341. https://doi.org/10.1175/JCLI-D-16-0434.1

Yeh, S. W., Kug, J. S., Dewitte, B., Kwon, M. H., Kirtman, B. P., & Jin, F. F. (2009). El Niño in a changing climate. *Nature*, *461*(7263), 511–514. https://doi.org/10.1038/nature08316

Zhang, L., & Karnauskas, K. B. (2016). The role of tropical interbasin SST gradients in forcing Walker circulation trends. *Journal of Climate*, *30*(2), 499–508.

Zhang, W. J., Jin, F. F., Li, J. P., & Ren, H. L. (2011). Contrasting impacts of two–type El Niño over the western North Pacific during boreal autumn. *Journal of the Meteorological Society of Japan*, *89*(5), 563–569. https://doi.org/10.2151/jmsj.2011-510

Zhang, W. J., Jin, F. F., & Turner, A. (2014). Increasing autumn drought over southern China associated with ENSO regime shift. *Geophysical Research Letters*, *41*, 4020–4026. https://doi.org/10.1002/2014GL060130

Zhang, W. J., Jin, F. F., Zhao, J. X., Qi, L., & Ren, H. L. (2013). The possible influence of a nonconventional El Niño on the severe autumn drought of 2009 in southwest China. *Journal of Climate*, *26*(21), 8392–8405. https://doi.org/10.1175/JCLI-D-12-00851.1

Zhang, W. J., Li, J. P., & Zhao, X. (2010). Sea surface temperature cooling mode in the Pacific cold tongue. *Journal of Geophysical Research*, *115*, C12042. https://doi.org/10.1029/2010JC006501

Zhang, Y., Li, J., Xue, J., Feng, J., Wang, Q., Xu, Y., et al. (2018). Impact of the South China Sea summer monsoon on the Indian Ocean dipole. *Journal of Climate*, *31*(16), 6557–6573. https://doi.org/10.1175/JCLI-D-17-0815.1

Zheng, F., Fang, X. H., Yu, J. Y., & Zhu, J. (2014). Asymmetry of the Bjerknes positive feedback between the two types of El Niño. *Geophysical Research Letters*, *41*, 7651–7657. https://doi.org/10.1002/2014GL062125

Zheng, F., Fang, X. H., Zhu, J., Yu, J. Y., & Li, X. C. (2016). Modulation of Bjerknes feedback on the decadal variations in ENSO predictability. *Geophysical Research Letters*, *43*, 12,560–12,568. https://doi.org/10.1002/2016GL071636

Zheng, F., Li, J. P., Ding, R. Q., & Feng, J. (2017). Cross-seasonal influence of the SAM on Southern Hemisphere extratropical SST and its relationship with meridional circulation in CMIP5 models. *International Journal of Climatology*, *38*(3), 1499–1519. https://doi.org/10.1002/joc.5262

Zheng, F., Li, J. P., Feng, J., Li, Y. J., & Li, Y. (2015). Relative importance of the austral summer and autumn SAM in modulating Southern Hemisphere extratropical autumn SST. *Journal of Climate*, *28*(20), 8003–8020. https://doi.org/10.1175/JCLI-D-15-0170.1

Zheng, F., Li, J. P., Wang, L., Xie, F., & Li, X. F. (2015). Cross-seasonal influence of the December–February Southern Hemisphere annular mode on March–May meridional circulation and precipitation. *Journal of Climate*, *28*(17), 6859–6881. https://doi.org/10.1175/JCLI-D-14-00515.1